Patched, the receptor of Hedgehog, is a lipoprotein receptor

Ainhoa Callejo, Joaquim Culi*, and Isabel Guerrero†

Centro de Biología Molecular ''Severo Ochoa,'' Universidad Autónoma de Madrid, Cantoblanco, E-28049 Madrid, Spain

The Hedgehog (Hh) family of secreted signaling proteins has a broad variety of functions during metazoan development and implications in human disease. Despite Hh being modified by two lipophilic adducts, Hh migrates far from its site of synthesis and programs cellular outcomes depending on its local concentrations. Recently, lipoproteins were suggested to act as carriers to mediate Hh transport in *Drosophila*. Here, we examine the role of lipophorins (Lp), the *Drosophila* lipoproteins, in Hh signaling in the wing imaginal disk, a tissue that does not express Lp but obtains it through the hemolymph. We use the up-regulation of the Lp receptor 2 (LpR2), the main Lp receptor expressed in the imaginal disk cells, to increase Lp endocytosis and locally reduce the amount of available free extracellular Lp in the wing disk epithelium. Under this condition, secreted Hh is not stabilized in the extracellular matrix. We obtain similar results after a generalized knock-down of hemolymph Lp levels. These data suggest that Hh must be packaged with Lp in the producing cells for proper spreading. Interestingly, we also show that Patched (Ptc), the Hh receptor, is a lipoprotein receptor; Ptc actively internalizes Lp into the endocytic compartment in a Hh-independent manner and physically interacts with Lp. Ptc, as a lipoprotein receptor, can affect intracellular lipid homeostasis in imaginal disk cells. However, by using different Ptc mutants, we show that Lp internalization does not play a major role in Hh signal transduction but does in Hh gradient formation.

Drosophila | LDLR | morphogen

The Hedgehog (Hh) family of signaling molecules organizes spatial patterning in a wide variety of morphogenetic processes in both insects and vertebrates (1–3). Hh proteins act as morphogens during development: Hh proteins spread from localized sites of production to specify a diverse array of cell fates, ranging from segmental patterns in the *Drosophila* embryo to neurons in the vertebrate neural tube, in a concentration-dependent manner (reviewed in refs. 4 and 5). Hh also plays an important role in the maintenance and regulation of stem cells in adult organisms (6–8). Abnormal activation of the Hh signaling pathway has been implicated in the initiation and growth of many human tumors (9).

The mature Hh protein is synthesized as a precursor that undergoes a series of posttranslational modifications, leading to the covalent attachment of a cholesterol moiety at its carboxyl-terminus and palmitic acid at its amino terminus (10). These lipid adducts confer to Hh a high affinity for cell membranes (11, 12). Despite this, Hh protein can signal to cells distant from the source of its production (3). The spreading of Hh is a highly regulated process and is a critical determinant of morphogen gradient formation. The hydrophobic nature of lipid-modified Hh has significant effects on the shape and range of its activity gradient. Indeed, expression of different forms of Hh that lack either the cholesterol moiety (Hh-N or Shh-N) or the palmitic acid (HhC85S or ShhC25S) in several animal models led to profound alterations in the spreading and signaling properties of Hh. The emerging theme is that the cholesterol and palmitate moieties help generate a steep Hh gradient across the extracellular matrix of a morphogenetic field by restricting Hh dilution

and unregulated diffusion (13). In this context, it has been described that the HSPGs and Shifted, a component of the extracellular matrix, are important for stabilization and spreading of only the lipid-modified Hh (14–20).

The range of the Hh gradient is also limited by endocytosis mediated by the Hh receptor Patched (21–24). Genetic studies indicate that up-regulation of Ptc in Hh-receiving cells functions to sequester Hh, creating a barrier to further movement and thereby limiting the range of Hh action (21). Localization of Ptc in multivesicular bodies and endosomes (24, 25) and its removal from the plasma membrane upon exposure to Hh (24, 26, 27) support the hypothesis that Ptc scavenges Hh by transporting it through the endocytic pathway.

At least two models have been proposed to explain how the lipophilic Hh can spread through an aqueous tissue. Fractionation studies of the supernatant of Hh-expressing cells showed that Hh participates in high molecular weight structures that probably represent multimeric complexes, and cholesterol and palmitic acid seems to mediate this multimerization (12, 19, 28, 29). The lipid moieties are thought to be embedded in the core of these complexes, in analogy to micelles. Recently, a second model was proposed: it suggests that lipoprotein particles could carry lipid-modified ligands such as Hh and Wingless, acting as vehicles for long-range transport. Vertebrate lipoprotein particles are scaffolded by apolipoproteins and consist of a phospholipid monolayer surrounding a core of esterified cholesterol and triglycerides. Insects form similar particles that are called Lipophorins (Lp) and contain Apolipophorins I and II (ApoLI and ApoLII) (30, 31). These proteins are produced in the fat body (32) by cleavage of the precursor pro-Apolipophorin (32, 33), and are not synthesized by imaginal disk cells (34) but receive them through the hemolymph. Panakova *et al.* (34) described that a systemic reduction of lipoprotein levels in the hemolymph, by expression of Lp (ApoLI-II) RNAi in the fat body, affects long-range but not short-range Hh signaling. They also found that Wnt and Hh proteins copurify with lipoproteins from tissue homogenates and colocalize with lipoprotein particles in the developing wing epithelium. More recently, an interaction between Lp and the glypicans, Dally and Dally-like, has been found (35).

Here, we have tested the role of lipoproteins in Hh signaling. To this aim, we knocked down the lipoprotein gene by RNA interference, reducing Lp supply in the hemolymph. In addition, we locally reduced the amount of extracellular Lp in the wing imaginal disk cells by overexpressing Lipophorin receptor 2

(LpR2), which increases Lp endocytosis. Under both experimental conditions we observe a decrease in extracellular Hh. These results suggest an important role of lipoproteins in Hh anchoring and spreading through the extracellular matrix. Moreover, we have observed that Ptc actively internalizes Lipophorins, effectively acting as a Lipoprotein receptor, and that its over-expression can alter intracellular lipid homeostasis. Collectively, our results are consistent with the model of lipoprotein particles acting as vehicles for Hh transport.

Results and Discusion

Lipophorins Are Required for Extracellular Hh Stability. To study the requirement of Lp in Hh signaling, we first analyzed a null ApoL mutant (RfaBp^{C204}). This mutant is embryonic lethal. However, the homozygous embryos do not show a segmentation phenotype related to the Hh pathway. This is not surprising, because the early embryos contain high amounts of maternal ApoLI-II proteins that could mask an early requirement of Lp in Hh signaling (data not shown). Later during development, we observed that *apoLI-II* genes are transcribed in the fat body (Fig. 1*B* and ref. 32) and not in imaginal discs (Fig. 1*A*), but apoLI and ApoLII proteins can be detected both in the fat body (Fig. 1*C*) and also in imaginal discs (Fig. 1*D*). To analyze the requirement of Lp in Hh transport in the imaginal disk cells, we first reduced the Lp supply by expressing ApoLI and ApoLII RNAi in the fat body. We observed that this severe reduction of ApoLI-II has a pleiotropic effect in all tissues and organs, affecting also the viability of the larvae (data not shown). To overcome this problem, we transiently expressed the RNAi transgene using a heat-shock-inducible promoter. Two pulses of Lp RNAi expression before disk dissection caused a decrease in Lp levels in the imaginal discs (Fig. 1*E*, compare with Fig. 1*D* and graph in Fig. 1*K*) and also a reduction of Hh levels in the P compartment of the wing imaginal disk (Fig. 1*G*, compare with Fig. 1*F* and graph in Fig. 1*J*), affecting also the range of all Hh responses (Fig. 1*I* compare with Fig. 1*H*, plots in Fig. 1*L* and data not shown). These results are in disagreement with Panakova *et al.* (34), who found that, in lipophorin–RNAi discs, Hh accumulates to abnormally high levels in the first five rows of anterior cells, affecting long- but not short-range Hh signaling.

To analyze Lp requirement in the imaginal disk cells in more detail, we reasoned that another way to reduce the amount of Lp in the extracellular space of the wing imaginal disk was to ectopically express LpR2, one of the two LpR in the fly, to increase Lp internalization and locally remove it from the extracellular space. However, long-term ectopic expression of LpR2 induces apoptosis (data not shown). To prevent the cell lethality issue we used the Gal4/Gal80^{ts} system. A pulse at the restrictive temperature inactivates the repressor Gal80 protein, allowing the Gal4 protein to activate *UAS-lpr2*. When LpR2 was transiently expressed for 24 h in the dorsal compartment of the wing discs, we did not observe expression of activated Caspase 3, an apoptotic marker [supporting information (SI) Fig. 5*A*]. As expected, LpR2 overexpression increased endocytosis of Lp, as indicated by the accumulation of Lp-containing intracellular vesicles (Fig. 2*A*, *Inset*). Interestingly, ectopic LpR2 also caused a decrease in the total amount of Hh (Fig. 2*B*, and chart in *D*) and in all Hh readouts (data not shown), as we had previously observed by Lp knockdown using RNAi (Fig. 1 *D–K*). The observed decrease in Hh levels occurs mainly in the extracellular space (Fig. 2*C*). We then set out to analyze in which step of the Hh production machinery (transcription, secretion, or transport/extracellular stability) ectopic LpR2 was interfering with. Using *hh-LacZ* as a reporter we observed no transcriptional variation (SI Fig. 6*B*). To analyze whether overexpressed LpR2 was interfering with Hh transport to the cell membrane, we made use of the fact that in clones of cells lacking Disp function, Hh release is
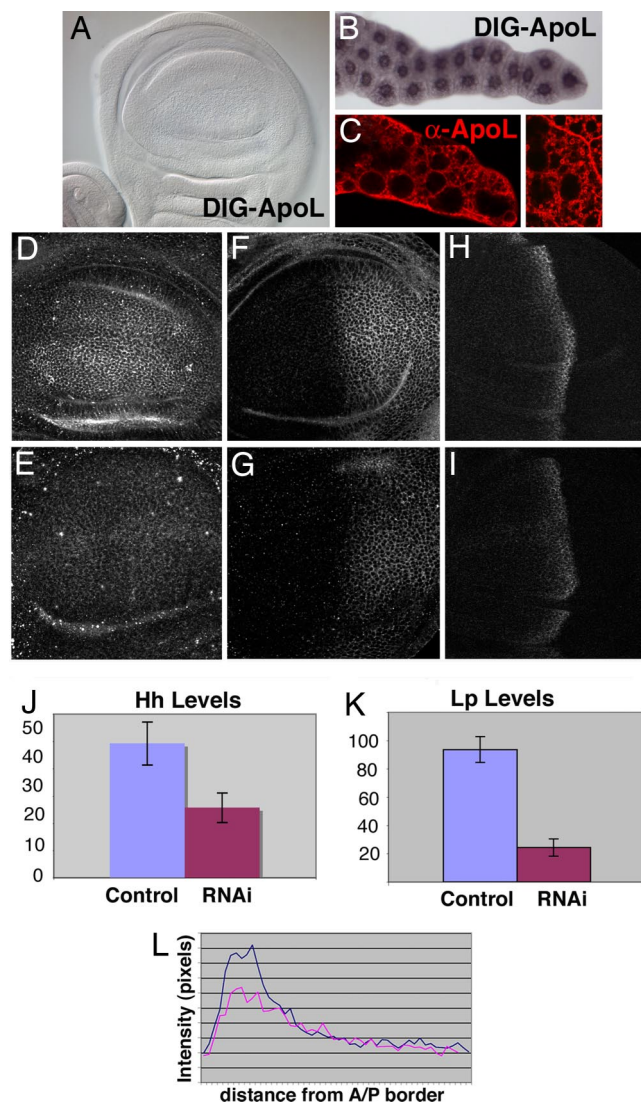

Fig. 1. Systemic Reduction of Lp decreases Hh levels in the wing imaginal disk. (*A* and *B*) *In situ* hybridization using an antisense-ApoLI-II probe in a wing disk (*A*) and in the fat body (*B*) of wild-type larvae. (*C*) Fat body cells immunostained with the anti-ApoLI-II antibody. Note the accumulation of ApoLI-II protein in vesicular structures (*Inset*). (*D–I*) Expression of Lp (*D* and *E*), Hh (*F* and *G*), and Ptc (*H* and *I*) in control *HS-Gal4* wing imaginal discs (*D, F*, and *H*) and in wing discs of a *HS-Gal4*; *UAS-LpRNAi* larvae (*E, G*, and *I*). Both control and RNAi larvae were similarly heat-shocked before dissection. Note the decrease in Hh and Ptc levels. (*J*) Graph representing Hh levels in *HS-Gal4* wing discs (control) and in wing discs of a *HS-Gal4*; UAS-LpRNAi larvae (average of six discs, error bars represent standard deviations). (*K*) Graph representing Lp levels in *HS-Gal4* wing discs (control) and in wing discs of a *HS-Gal4*; UAS- LpRNAi larvae (average of six discs, error bars represent standard deviations). (*L*) Plots showing Ptc fluorescence intensity along the A/P axis in wild-type wing disk (blue line) or in a wing disk of a *HS-Gal4*; *UAS-LpRNAi* larvae (pink line).

blocked and thus, accumulate Hh at the plasma membrane (36). This accumulation occurs in the extracellular side of the baso-lateral plasma membrane (SI Fig. 6*D*; A.C., N. Gorfinkiel, and I.G., unpublished results). Overexpression of LpR2 in these *disp⁻* cells, using the MARCM system, still showed Hh accumulation, indicating that LpR2 overexpression does not interfere with Hh transport to the cell surface (SI Fig. 6*C* compared with SI Fig. 6*D* and ref. 36). We then analyzed whether the decrease in extracellular Hh levels was caused by endocytosis and lysosomal degradation of the protein after
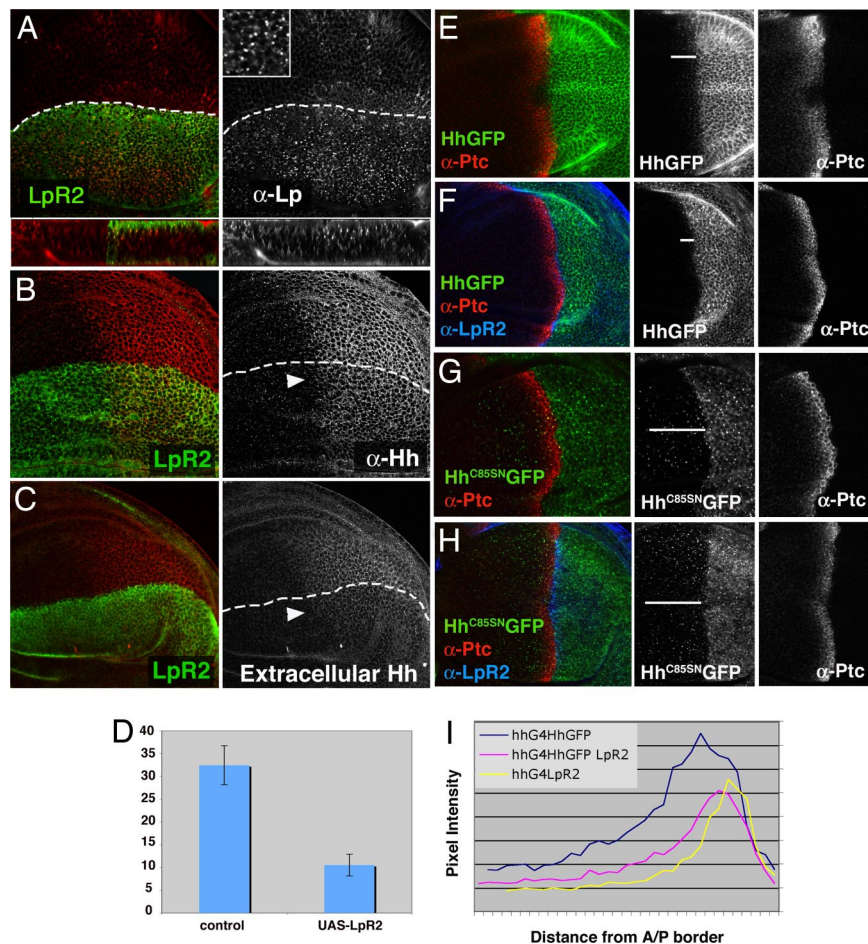
Fig. 2. Ectopic LpR2 in the wing imaginal discs increases Lp internalization and reduces extracellular Hh levels. (*A*) Immunostaining of *ap-Gal4*; *TubGal80^ts^/UAS-LpR2-HA* wing disk (24 h at the restrictive temperature) using anti-HA antibody to show ectopic LpR2 expression (green) and anti-ApoLI-II antibody in red and gray (*Upper Inset*). Note the accumulation of ApoLI-II in punctuated structures in the dorsal compartment. Transversal sections show ApoLI-II localization in apical, lateral, and basal region of cells and in endocytic vesicles. (*B*) Immunostaining of a similar disk with anti-HA (LpR2, green) and anti-Hh antibody (red and gray). Observe the reduction of Hh levels in the dorsal-posterior compartment (arrowhead). (*C*) Extracellular immunostaining of a similar disk with anti-Hh antibody showing a striking decrease in extracellular Hh (red and gray) caused by ectopic LpR2 (anti-HA, green). Arrowhead points to the posterior-dorsal compartment. (*D*) Chart representing Hh inmunofluorescence intensity of ventral (control) versus dorsal compartments of 26 *UAS-LpR2-HA/ap-Gal4*; *TubGal80^ts^* wing discs. (*E*) *TubGal80^ts^/hh-Gal4, Hh-GFP* wing disk (24 h at the restrictive temperature) immunostained with anti-Ptc (red and gray). Observe that a gradient of Hh-GFP (green and gray) can be observed in the A compartment (white bar). (*F*) *TubGal80^ts^*; *hh-Gal4, Hh-GFP/UAS-LpR2-HA* wing disk immunostained with anti-Ptc antibody (red) and anti-HA to detect the expression of LpR2 (blue). Note that Hh levels in the P compartment, the Hh gradient (white bar) and Ptc expression are reduced compared with *E*. (*G*) Immunostaining with anti-Ptc antibody (red) of a *TubGal80^ts^/UAS-HhC85SN-GFP*, *hh*-Gal4 wing disk, which overexpresses a form of Hh (green and gray) without both palmitic acid and cholesterol. (*H*) Immunostaining with anti-HA (LpR2, blue) and anti-Ptc (red) antibodies of a *TubGal80^ts^*; *UAS-HhC85SN-GFP, hh-Gal4/UAS-LpR2-HA* wing disk. Observe that LpR2 overexpression does not alter HhC85SN-GFP levels (green and gray) in the P compartment nor modifies its gradient in the A compartment. (*I*) Chart showing the variation in Ptc fluorescence intensity along the A/P axis in *TubGal80^ts^*; *hh-Gal4, Hh-GFP* wing discs (an average of 12 discs, blue line), in *TubGal80^ts^*; *hh-Gal4, Hh-GFP/UAS-LpR2-HA* wing discs (an average of 10 discs, pink line) and in *TubGal80^ts^*; *hh-Gal4/UAS-LpR2-HA* wing discs (an average of five discs, yellow line).

secretion. We made use of the *shibire^ts1^* (*shi^ts1^*) mutant, which is a temperature-sensitive *dynamin* mutant, which blocks the fission of clathrin-coated vesicles and the internalization of caveolae (revised in ref. 37). We ectopically expressed LpR2 in a *shi^ts1^* mutant background. Under these conditions, we could still observe a decrease in extracellular Hh levels in the posterior compartment (SI Fig. 6E), suggesting that this reduction is not due to increased internalization and degradation of Hh after secretion. Taken together, these results indicate that Lp are required for Hh stabilization in the extracellular matrix, possibly by allowing the packaging of Hh into lipoprotein particles. If this is the case, we should expect that the lipidic Hh adducts would be essential in mediating this effect. In fact, LpR2 expression did not destabilize a nonlipidated Hh-GFP protein when coexpressed in the P compart-

ment (Fig. 2 *G* and *H*). On the contrary, a lipidated Hh-GFP fusion protein responded to LpR2 overexpression like endogenous Hh, showing decreased levels in the P compartment (Fig. 2 *E* and *F*) and a shorter Hh-GFP gradient in the A compartment (Fig. 2 *E* and *F*, and plot in Fig. 2*I*). Similar specific destabilization of lipid modified Hh in the extracellular matrix has been observed both in *HSPG* and *shf* mutants (15–20). All together these results suggest that Hh lipid modifications are necessary for Hh packaging with Lp to interact with the extracellular matrix components or that Lp could stabilise the binding of Hh to HSPGs.

To investigate whether altered Lp levels can also affect reception of the Hh signal and not only its secretion, we overexpress LpR2 exclusively in the receiving cells using the *ptc-Gal4* driver. We found that the Hh gradient was slightly
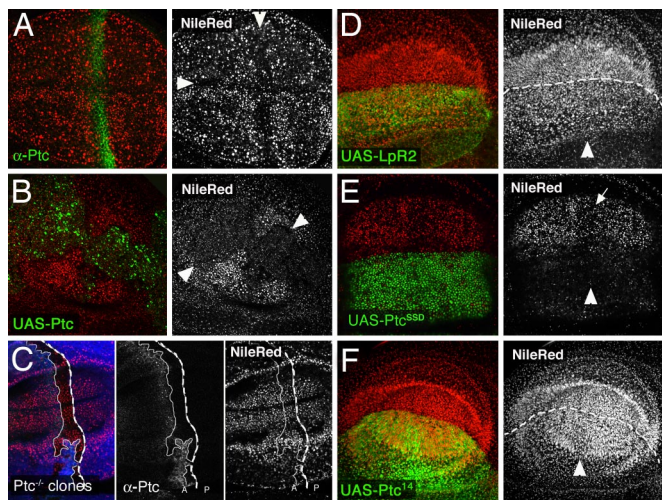
expanded compared with wild-type discs. For example, expression of Ptc and Engrailed (En) were extended a few cell diameters into the anterior compartment (SI Fig. 7). LpR2 overexpression in the receiving cells probably decreases Hh endocytosis by its receptor Ptc, thereby increasing the range of the Hh gradient. However, how LpR2 interacts with the Hh reception machinery needs to be clarified.

Ptc as a Lipoprotein Receptor. Because Hh seems to be associated to lipoprotein particles, it was expected that a member of the LDLR family could modulate the response to Hh or interact with Ptc. In the case of Wg, another lipid modified signal, the LDLR protein Arrow (LDLR5/6) is required for Wg signaling in addition to the serpentine receptors Frizzled (38, 39). The most obvious candidate was the LpR; however, *lpr1* and *lpr2* null mutants are homozygous viable with no wing pattern alterations (J.C., unpublished observations). Moreover, we have not found a genetic interaction between *lpr1/2* and mutations in the Hh pathway with the exception of the described effect of overexpressed LpR2 (Fig. 2 and SI Fig. 7). In addition, we have analyzed whether Megalin (CG34352), another member of the LDLR, which was found to internalize Shh in mammalian tissue culture cells (40), was involved in Hh sequestration in *Drosophila*. However, our data indicate that Megalin is not involved either in reception or in internalization of Hh (unpublished results). Because no LDLR seems to be involved in Hh reception, we tested whether Ptc itself was able to directly interact with the lipoprotein particles. To investigate this possibility, we ectopically and transiently expressed Ptc in wing discs using the Gal80^{ts}/Gal4 system in the dorsal compartment of the discs. After 24 h at the restrictive temperature we observed that overexpressed Ptc actively internalized Lp (Fig. 3B). We found a high percentage of colocalization of Hh, Ptc and ApoLs in early endocytic vesicles (Fig. 3 A, B, and Insets), when we labeled with anti-AP-2 antibody (AP50) (Fig. 3C), which labels the AP-2 adaptor complex involved in clathrin-mediated endocytosis (41). We also observed a colocalization of Ptc and ApoLs with the late endosomes markers Hrs (42) (Fig. 3D) and Rab7-GFP (43) (Fig. 3E). However, this ability of Ptc to internalize Lp is independent of the presence of Hh, as it was shown by the endocytosis of Lp in cells far from the A/P compartment border, where there is no Hh. Moreover, in discs not overexpressing Ptc, we still observe a strong colocalization of ApoL, Hh and Ptc in endocytic vesicles of anterior cells, particularly in their most apical domain, where early endosomes accumulate (Fig. 3A). Because Ptc efficiently internalizes Lp, we then asked whether there was a molecular interaction between Ptc and ApoLI-II in immunoprecipitation studies. ApoLI protein was immunoprecipitated by Ptc in salivary glands overexpress-

Fig. 3. Ptc interacts with Lp and induces its internalization. (A) *hh-Gal4/UAS-Hh-GFP* wing disk immunostained with anti-Ptc (blue) and anti-ApoLI-II antibody (red) to show the colocalization at the A/P compartment border of Hh-GFP (green), Ptc, and ApoL in punctuated apical structures. (B) *Ap-Gal4/UAS-Ptc^{WT}-GFP*; *TubGal80^{ts}* wing disk (incubated 24 h at the restrictive temperature) accumulates Lp (ApoLI-II) (red), Ptc-GFP (green), and Hh (blue) in punctuated structures (*Inset*, yellow arrowheads point to colocalization). (C–E) Colocalization of Lp (ApoLI-II) (red) and Ptc (green in C and D and blue in E) with AP50 (blue, C) a marker of the early endocytic compartment (arrowheads), Hrs (blue, D), and with Rab7-GFP (green, E) both markers of the late endocytic compartment in *Ap-Gal4*; *TubGal80^{ts}/UAS-Ptc^{WT}* wing disk (24 h at the restrictive temperature) (arrowheads). (F) *Ap-Gal4/UAS-Ptc^{SSD}-GFP*; *TubGal80^{ts}* wing disk (24 h at the restrictive temperature) immunostained with anti-Hh (blue) and anti-ApoLI-II (red) antibodies. Note that Ptc^{SSD}-GFP (green, Ptc^{SSD} has a mutation in its SSD domain) expressing cells also accumulate both Lp (ApoLI-II) and Hh. (G) *Ap-Gal4/UAS-Ptc^{14}-GFP*; *TubGal80^{ts}* wing disk (24 h at the restrictive temperature). Overexpression of Ptc^{14}-GFP mutant protein, which is endocytosis-defective, is not able to induce internalization of neither Lp (ApoLI-II) (red) nor Hh (blue) protein. (H) Immunoprecipitation (IP) and Western blot assays: Mw, molecular weight markers; lane IP^1, IP of a protein extract from larvae of *UAS-Ptc^{WT}-GFP*; *AB1Gal4* genotype using anti-GFP (mouse) and developed with anti-ApoLI-II (rabbit). Observe a band >200 kDa (arrowhead) that correspond to the ApoLI higher molecular weigh subunit; lane input: a fraction of the same lysate. Observe two bands, one of 200 kDa (Apo-LI) and another of 75 kDa (Apo-LII), which correspond to each of the two Lp monomers; lane IP^2, IP of a protein extract from *UAS-Ptc^{WT}-GFP*; *AB1Gal4* larvae using anti-GFP (mouse) and developed with anti-GFP (rabbit). Observe a band near 200 kDa that corresponds to Ptc-GFP; lane IP^C (negative control): IP of protein extract of wild-type salivary glands using anti-GFP mouse and detected with anti-ApoLI-II. The bands at ≈55 kDa in lanes IP^1, IP^2, and IP^C correspond to IgG.

Fig. 4. Ptc regulates intracellular lipid homeostasis. (*A*) Wild-type wing disk stained with NileRed (red) and anti-Ptc (green). Note a reduction in lipid droplets at the A/P and D/V compartment borders (arrowheads). This reduction is more pronounced at the subapical part of the epithelia. (*B*) Wing imaginal discs expressing ectopic Ptc^WT-GFP (green) in clones (arrowheads) and stained with NileRed dye. Note the reduction of lipid droplets inside the clones. (*C*) Wing disk containing *ptc^16* (a null allele) clones, marked by the lack of armLacZ (blue), and stained with NileRed dye (red and gray) and anti-Ptc (green and gray). Although these clones activate the Hh pathway, they do not express Ptc protein, and therefore, do not reduce the amount of lipid droplets. (*D*) *UAS-LpR2-HA/ap-Gal4*; *TubGal80^ts* wing disk (24 h at the restrictive temperature). Note the reduction of lipid droplets, shown by nile red staining, in the dorsal compartment (arrowhead). (*E*) *ap-Gal4/UAS-Ptc^SSD-GFP*; TubGal80^ts wing disk (24 h at the restrictive temperature) similarly stained with NileRed dye. Note a decrease in the lipid droplets in the A/P border and in the dorsal compartment (arrowhead). (*F*) *ap-Gal4/UAS-Ptc^14-GFP*; *TubGal80^ts* wing disk (24 h at the restrictive temperature) stained with NileRed dye. Note that the lipid droplets do not decrease in the dorsal compartment (arrowhead).

ing Ptc-GFP (Fig. 3*H*). These assays confirm the physical interaction between these two proteins.

To test whether internalization of Lp was important for Smo regulation we made use of two Ptc mutants. Ptc^SSD contains a mutation in its sterol-sensing domain (SSD) that, by analogy to other SSD-containing proteins, can make the protein insensitive to modulation by sterols (44). It has been found that this mutant cannot repress Smo function, activating the Hh pathway, but is still able to internalize Hh (45, 46). After ectopic expression of Ptc^SSD (Ptc^S2), we observed Lp internalization at a higher degree than when using Ptc^WT (Fig. 3*F*). Therefore, both wild-type Ptc, which blocks the Hh pathway, and Ptc^SSD, which constitutively activates the pathway, internalize Lp, indicating that this is a property of Ptc independent of its function in Hh signal transduction. The second Ptc mutant we used was Ptc^14, which regulates Smo in response to Hh but is defective in Hh endocytosis (24). Here, we found that ectopic Ptc^14 was not able to internalize Lp (Fig. 3*G*). These data indicate that internalization of Lp is not absolutely required for normal Smo modulation, as we had previously suggested for Hh internalization (24). Therefore, although lipoprotein particles are important for both Hh transportation through the extracellular matrix and to control the Hh gradient, internalization of Lp plays a minor role in Hh signal transduction.

Because Ptc can act as a Lipoprotein receptor, we asked whether it was able to modulate lipid homeostasis. Unexpectedly, a down-regulation in lipid droplets was also observed at the A/P and D/V compartment borders in wild-type discs (Fig. 4*A*), where either Hh or Wg reception takes place. This data suggests that Ptc can affect the amount of intracellular lipid droplets. In fact, in *ptc^16* mutant clones, which do not produce Ptc protein at

the A/P compartment border, we were unable to observe a down-regulation of lipid droplets (Fig. 4*C*) and ectopic Ptc clones induced early in development and maintained for several days induced a marked decrease in the accumulation of intracellular lipid droplets (Fig. 4*B*). Using an apoptotic marker (anti-activated Caspase 3 antibody), we showed that the down-regulation in lipid droplets was not consequence of apoptosis (SI Fig. 5*B*). Why the massive endocytosis of lipoproteins induced by Ptc results in a decrease instead of a rise in the amount of lipid droplets is not clear. However, we have observed that overexpression of the LpR2 similarly reduced intracellular lipid droplets (Fig. 4*D*). The down-regulation of lipid droplets was also observed after transiently expressing Ptc^SSD for 24 h in the dorsal compartment of the wing imaginal disk, which constitutively activates the Hh pathway (Fig. 4*E*). However, we did not observe the same effect in either ectopic expression of Ptc^14 (Fig. 4*F*) that does not internalize Lp. Because the same effect in the amount of lipid droplets was observed with both wild-type Ptc, which blocks the Hh pathway, and with Ptc^SSD, which constitutively opens the pathway, but not by the activation of the pathway in the absence of Ptc protein, we concluded that the effect of Ptc in lipid metabolism is an aspect of Ptc function independent of its role in the Hh signal transduction.

Previous observations have indicated that both in *Drosophila* and mammalian models, fat-body-specific transgenic activation of Hh signaling inhibits fat-body formation (47). Conversely, fat-body-specific inhibition in Hh signal stimulated fat-body formation. In mammals, sufficiency and necessity tests showed that Hh signaling also inhibits adipogenesis (47). These data support the notion that Hh signaling plays a conserved role, from invertebrates to vertebrates, in inhibiting fat formation. Here, we found that Ptc, *per se*, and not Hh signaling inhibits intracellular lipid droplet accumulation, a process reminiscent of fat body differentiation. Because Ptc is also a target of the Hh pathway, our results suggest the possibility that the described anti-adipogenic activity of the Hh pathway may in part be mediated by the activation of Ptc. Our results highlight the potential of Ptc as a therapeutic target for osteoporosis, lipodystrophy, diabetes, and obesity.

Concluding Remarks

Here we have made advances in the understanding of the mechanism of Hh spreading testing the role played by lipoprotein particles as vehicles for long-range Hh transport. We show that depleting the amount of free Lp in the extracellular space, either by ectopic expression of the LpR2 or by knocking down the Lp supply in the hemolymph, results in a decrease in the stability of extracellular Hh. We also demonstrate that ectopic expression of Ptc causes internalization of Lp into the endocytic compartment in a Hh-independent way. However, how the role of Ptc as a Lp receptor correlates with its activity in the regulation of the Hh pathway needs further analysis. Finally, we show that Ptc modulates intracellular lipid homeostasis independently of its role in the regulation of the Hh pathway. These results open new ways of exploring the mechanism of Hh signaling, linking Hh to lipid metabolism, and have broad implications in the treatment of tumors.

Materials and Methods

Overexpression Experiments and Generation of Clones. We used the following *Drosophila* stocks: *UAS-LpRNAi* was obtained from IMP Vienna *Drosophila* RNAi Center (VDRC, Vienna, Austria), *Fat-body-Gal4* (48), *UAS-HhGFP* (24), and *UAS-HhC85SN-GFP* (19). To make the *UAS-LpR2* transgene, a full-length *LpR2* cDNA (EST line GH26833, obtained from Berkeley *Drosophila* Genome Project, Berkeley, CA) was fused in frame to a C-terminal HA tag and cloned into pUAST vector.

Transient expression of the UAS constructs using *ap-Gal4* (or *ptc-Gal4*); *Tub Gal80ts* was achieved by maintaining the crosses at 18°C and inactivating the Gal80ts repressor for 16–24 h at the restrictive temperature (29°C).

Mutant Clones. Clones were generated by *FLP*-mediated mitotic recombination. Larvae of the corresponding genotypes were incubated at 37°C for 1 h at 24–48 h after egg laying (AEL). The genotypes used were: *FLP; FRT 42D, ptc16/FRT 42D, arm-lacZ* and *FLP; FRT 82, dispS037707/FRT 82, ubi-GFP*.

Flip-Out Clones. The transgene *ubx>f+>Gal4, UAS-βgal* (49) was used to generate ectopic expression clones of the UAS lines. Larvae of the corresponding genotypes were incubated at 37°C for 15 min to induce *HS-FLP* mediated recombination.

Lp Knockdown by RNAi. larvae containing the *UAS-LpRNAi* transgene and the *HS-Gal4* driver were heat-shocked twice for 30 min at 37°C, 2 h apart. They were dissected 5 h afterward. Control discs only contained the *HS-Gal4* driver and were similarly heat-shocked.

1. Nusslein-Volhard C, Wieschaus E (1980) Mutations affecting segment number and polarity in Drosophila. *Nature* 287:795–801.
2. Chiang C, *et al.* (1996) Cyclopia and defective axial patterning in mice lacking Sonic hedgehog gene function. *Nature* 383:407–413.
3. Ingham PW, McMahon AP (2001) Hedgehog signaling in animal development: Paradigms and principles. *Genes Dev* 15:3059–3087.
4. Torroja C, Gorfinkiel N, Guerrero I (2005) Mechanisms of Hedgehog gradient formation and interpretation. *J Neurobiol* 64:334–356.
5. Ingham PW, Placzek M (2006) Orchestrating ontogenesis: Variations on a theme by sonic hedgehog. *Nat Rev Genet* 7:841–850.
6. Zhang Y, Kalderon D (2001) Hedgehog acts as a somatic stem cell factor in the Drosophila ovary. *Nature* 410:599–604.
7. Lai K, Kaspar BK, Gage FH, Schaffer DV (2003) Sonic hedgehog regulates adult neural progenitor proliferation in vitro and in vivo. *Nat Neurosci* 6:21–27.
8. Palma V, Ruiz i Altaba A (2004) Hedgehog-GLI signaling regulates the behavior of cells with stem cell properties in the developing neocortex. *Development* 131:337–345.
9. Pasca di Magliano M, Hebrok M (2003) Hedgehog signalling in cancer formation and maintenance. *Nat Rev Cancer* 3:903–911.
10. Mann RK, Beachy PA (2004) Novel lipid modifications of secreted protein signals. *Annu Rev Biochem* 73:891–923.
11. Peters C, Wolf A, Wagner M, Kuhlmann J, Waldmann H (2004) The cholesterol membrane anchor of the Hedgehog protein confers stable membrane association to lipid-modified proteins. *Proc Natl Acad Sci USA* 101:8531–8536.
12. Gallet A, Ruel L, Staccini-Lavenant L, Therond PP (2006) Cholesterol modification is necessary for controlled planar long-range activity of Hedgehog in Drosophila epithelia. *Development* 133:407–418.
13. Guerrero I, Chiang C (2007) A conserved mechanism of Hedgehog gradient formation by lipid modifications. *Trends Cell Biol* 17:1–5.
14. Bellaiche Y, The I, Perrimon N (1998) Tout-velu is a Drosophila homologue of the putative tumour suppressor EXT-1 and is needed for Hh diffusion. *Nature* 394:85–88.
15. Bornemann DJ, Duncan JE, Staatz W, Selleck S, Warrior R (2004) Abrogation of heparan sulfate synthesis in Drosophila disrupts the Wingless, Hedgehog and Decapentaplegic signaling pathways. *Development* 131:1927–1938.
16. Takei Y, Ozawa Y, Sato M, Watanabe A, Tabata T (2004) Three Drosophila EXT genes shape morphogen gradients through synthesis of heparan sulfate proteoglycans. *Development* 131:73–82.
17. Glise B, *et al.* (2005) Shifted, the Drosophila ortholog of Wnt inhibitory factor-1, controls the distribution and movement of Hedgehog. *Dev Cell* 8:255–266.
18. Gorfinkiel N, Sierra J, Callejo A, Ibanez C, Guerrero I (2005) The Drosophila ortholog of the human Wnt inhibitor factor Shifted controls the diffusion of lipid-modified Hedgehog. *Dev Cell* 8:241–253.
19. Callejo A, Torroja C, Quijada L, Guerrero I (2006) Hedgehog lipid modifications are required for Hedgehog stabilization in the extracellular matrix. *Development* 133:471–483.
20. Gallet A, Rodriguez R, Ruel L, Therond PP (2003) Cholesterol modification of hedgehog is required for trafficking and movement, revealing an asymmetric cellular response to hedgehog. *Dev Cell* 4:191–204.
21. Chen Y, Struhl G (1996) Dual roles for patched in sequestering and transducing Hedgehog. *Cell* 87:553–563.
22. Gallet A, Therond PP (2005) Temporal modulation of the Hedgehog morphogen gradient by a patched-dependent targeting to lysosomal compartment. *Dev Biol* 277:51–62.
23. Incardona JP, Gruenberg J, Roelink H (2002) Sonic hedgehog induces the segregation of patched and smoothened in endosomes. *Curr Biol* 12:983–995.
24. Torroja C, Gorfinkiel N, Guerrero I (2004) Patched controls the Hedgehog gradient by endocytosis in a dynamin-dependent manner, but this internalization does not play a major role in signal transduction. *Development* 131:2395–2408.
25. Capdevila J, Estrada MP, Sanchez-Herrero E, Guerrero I (1994) The Drosophila segment polarity gene patched interacts with decapentaplegic in wing development. *EMBO J* 13:71–82.
26. Denef N, Neubuser D, Perez L, Cohen SM (2000) Hedgehog induces opposite changes in turnover and subcellular localization of patched and smoothened. *Cell* 102:521–531.
27. Zhu AJ, Zheng L, Suyama K, Scott MP (2003) Altered localization of Drosophila Smoothened protein activates Hedgehog signal transduction. *Genes Dev* 17:1240–1252.
28. Chen MH, Li YJ, Kawakami T, Xu SM, Chuang PT (2004) Palmitoylation is required for the production of a soluble multimeric Hedgehog protein complex and long-range signaling in vertebrates. *Genes Dev* 18:641–659.
29. Zeng X, *et al.* (2001) A freely diffusible form of Sonic hedgehog mediates long-range signalling. *Nature* 411:716–720.
30. Arrese EL, Gazard JL, Flowers MT, Soulages JL, Wells MA (2001) Diacylglycerol transport in the insect fat body: evidence of involvement of lipid droplets and the cytosolic fraction. *J Lipid Res* 42:225–234.
31. van der Horst DJ, van Hoof D, van Marrewijk WJ, Rodenburg KW (2002) Alternative lipid mobilization: the insect shuttle system. *Mol Cell Biochem* 239:113–119.
32. Kutty RK, *et al.* (1996) Molecular characterization and developmental expression of a retinoid- and fatty acid-binding glycoprotein from Drosophila: A putative lipophorin. *J Biol Chem* 271:20641–20649.
33. Sundermeyer K, Hendricks JK, Prasad SV, Wells MA (1996) The precursor protein of the structural apolipoproteins of lipophorin: cDNA and deduced amino acid sequence. *Insect Biochem Mol Biol* 26:735–738.
34. Panakova D, Sprong H, Marois E, Thiele C, Eaton S (2005) Lipoprotein particles are required for Hedgehog and Wingless signalling. *Nature* 435:58–65.
35. Eugster C, Panakova D, Mahmoud A, Eaton S (2007) Lipoprotein-heparan sulfate interactions in the Hh pathway. *Dev Cell* 13:57–71.
36. Burke R, *et al.* (1999) Dispatched, a novel sterol-sensing domain protein dedicated to the release of cholesterol-modified hedgehog from signaling cells. *Cell* 99:803–815.
37. van der Bliek AM (1999) Is dynamin a regular motor or a master regulator? *Trends Cell Biol* 9:253–254.
38. Wehrli M, *et al.* (2000) arrow encodes an LDL-receptor-related protein essential for Wingless signalling. *Nature* 407:527–530.
39. Tamai K, *et al.* (2000) LDL-receptor-related proteins in Wnt signal transduction. *Nature* 407:530–535.
40. McCarthy RA, Barth JL, Chintalapudi MR, Knaak C, Argraves WS (2002) Megalin functions as an endocytic sonic hedgehog receptor. *J Biol Chem* 277:25660–25667.
41. Ohno H, *et al.* (1995) Interaction of tyrosine-based sorting signals with clathrin-associated proteins. *Science* 269:1872–1875.
42. Lloyd TE, *et al.* (2002) Hrs regulates endosome membrane invagination and tyrosine kinase receptor signaling in Drosophila. *Cell* 108:261–269.
43. Entchev EV, Schwabedissen A, Gonzalez-Gaitan M (2000) Gradient formation of the TGF-beta homolog Dpp. *Cell* 103:981–991.
44. Kuwabara PE, Labouesse M (2002) The sterol-sensing domain: Multiple families, a unique role? *Trends Genet* 18:193–201.
45. Martin V, Carrillo G, Torroja C, Guerrero I (2001) The sterol-sensing domain of Patched protein seems to control Smoothened activity through Patched vesicular trafficking. *Curr Biol* 11:601–607.
46. Strutt H, *et al.* (2001) Mutations in the sterol-sensing domain of Patched suggest a role for vesicular trafficking in Smoothened regulation. *Curr Biol* 11:608–613.
47. Suh JM *et al.* (2006) Hedgehog signaling plays a conserved role in inhibiting fat formation. *Cell Metab* 3:25–34.
48. Gronke S, *et al.* (2003) Control of fat storage by a Drosophila PAT domain protein. *Curr Biol* 13:603–606.
49. de Celis JF, Bray S (1997) Feed-back mechanisms affecting Notch activation at the dorsoventral boundary in the Drosophila wing. *Development* 124:3241–3251.

DEVELOPMENTAL BIOLOGY